Test

Abstract

In this paper we investigated the radioactive decay of common radioisotopes and confirmed the attenuation coefficient dependence on energy and atomic number. The attenuation coefficients at 662keV and 1253 keV were found to agree with theory. The radioactivity of Brazilian and Ethiopian coffee was also studied, giving 880 ± 42Bq and 801 ± 35 Bq respectively, which is concordant with previous studies. The activity of a potassium chloride salt was measured to give a value of 12709 ± 80 Bq.

1 Introduction and Theory

Gamma ray spectrometers measure the intensity of incoming radiation with respect to their energy. Since γ radiation is high energy individual photons can be detected. Due to their versatility and ease of construction they have a wide spectrum of uses: from detecting radionuclides at nuclear facilities (it allows to classify the radioisotope rather than measuring the activity of it) to mapping interstellar objects such as stars and planets [1]. The basic principle of operation is identical and is independent on the application.

Out of the three types of ionising radiation (α, β, γ) gamma radiation has the lowest (comparing to α) ionising power and the highest energy (100keV+). Unlike β or α , γ radiation is a form of electromagnetic radiation and therefore has no mass(α particles can be treated as a helium ion of charge 2, β can be treated as an electron or positron). Gamma rays are produced by radioisotopes of commonly found materials, for example ^{137}Cs, ^{60}C ,^{22}Na are all radioisotopes which decay into stable elements by emitting radiation via emission of γ (and β) radiation at specific energies.

Due to the high energies associated with gamma rays, they are energetic enough to break covalent bonds in organic compounds,one of the reasons it is used to decontaminate medical equipment.

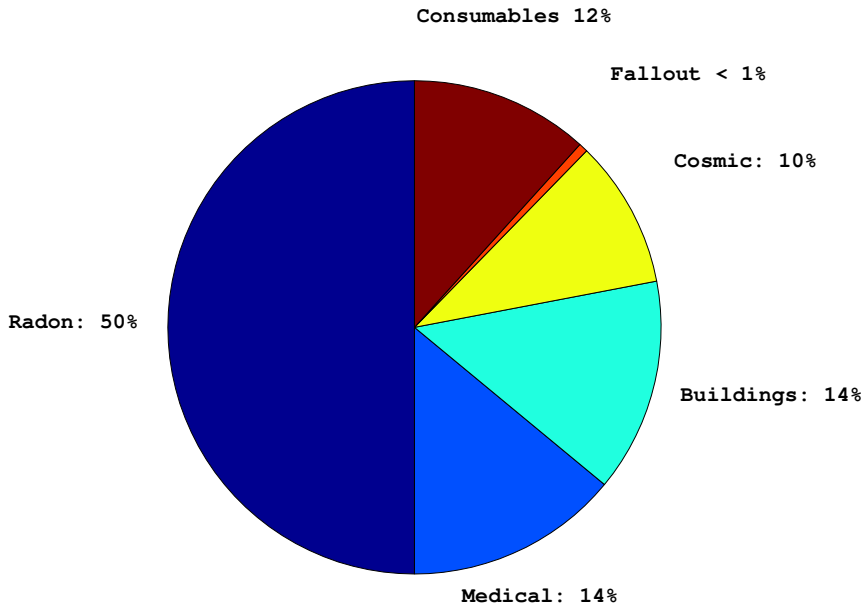

Figure 1: Pie chart of contributions to background data. Most of the background radiation comes from radon gas, followed by radioactivity found in buildings (^{60}Co in steel, amongst others), x-ray radiation from health services. Only a small proportion of the background radiation is attributed to radioactive fallout.

Radioactivity is a naturally occurring phenomenon found in every material. The majority of this background radiation originates from radon gas ($_{86}$Rn),

followed by isotopes found in building materials ($^{60}_{27}$Co is a common isotope found in steel) and foodstuffs ($^{40}_{19}$K) (Figure 1,page 2). Radioactivity occurs in unstable nuclei, whereby it emits radiation (α, β or γ) in an attempt to become stable. The cause of radioactivity is attributed to an inbalance in the proton-neutron count inside the atom, whereby the stable nuclei reside within the 'band of stability' and unstable nuclei outside. For light nuclei, the proton neutron ratio is roughly 1, increasing to ≈ 1.5 for heavier elements. Figure 2 summarises this.

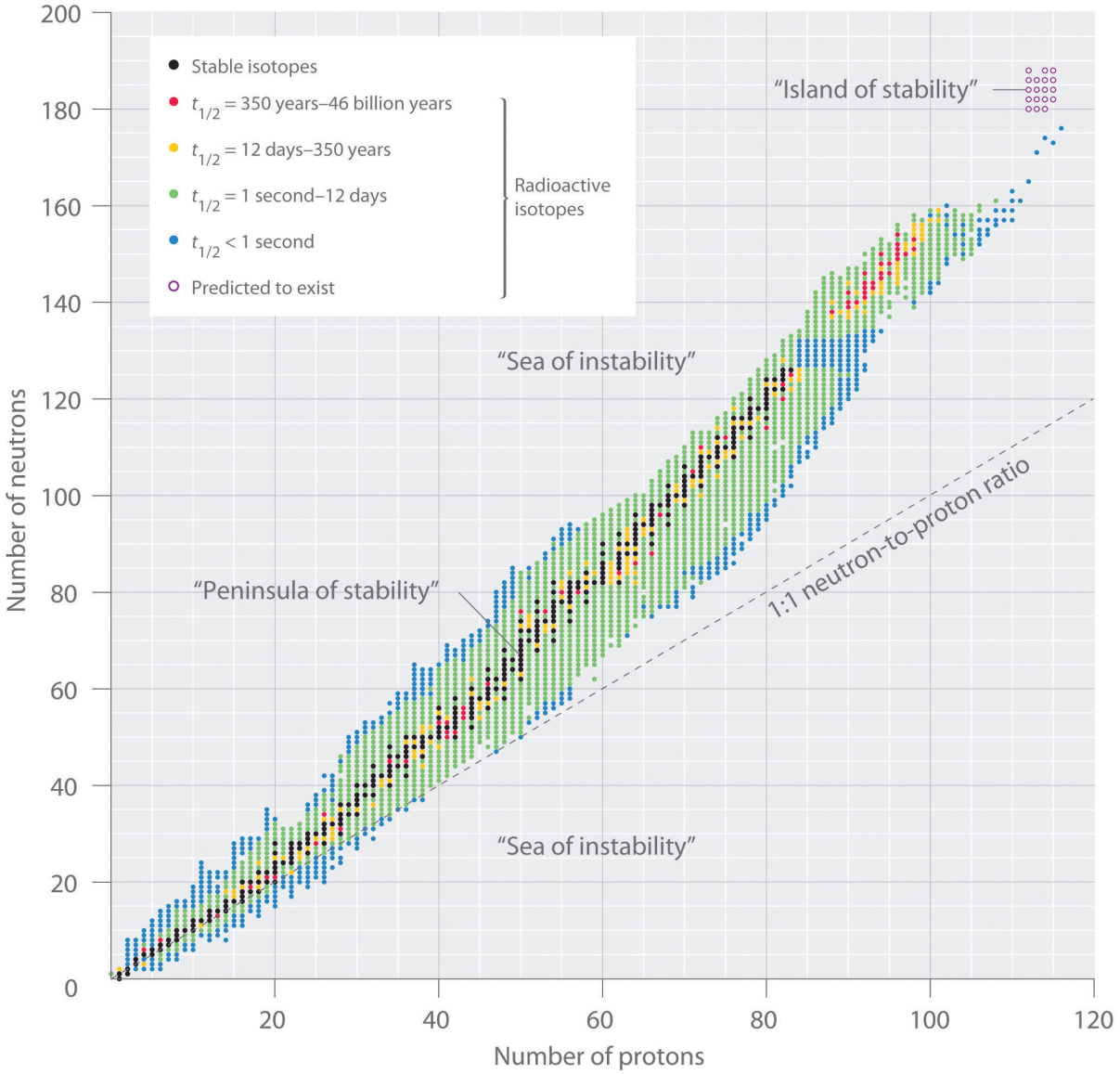

Figure 2: Diagram showing the 'band of stability', and other radioactive isotopes. blue blocks on the diagram represent $\beta-$ and $\beta+$ decay above and below the 'band of stability' [2].

This paper will attempt to confirm that increasing source energy, hv does not always increase the attenuation coefficient for a particular absorber. The energy of a gamma ray can be determined by equation 1

$$E = hf \tag{1}$$

where h is the Planck's constant and f is the frequency.
An alternative form of the above equation is

$$E = \frac{hc}{\lambda} \tag{2}$$

where λ is the wavelength of the gamma ray and c is the speed of light.
The attenuation coefficient for a particular material is given by equation 3,

$$I = I_0 \exp^{-\mu x} \tag{3}$$

where μ is the attenuation coefficient, x is the thickness, I_0 and I are the initial intensity and intensity respectively.

For this experiment a NaI(Sodium Iodide) scintillator coupled to an MCA (Multi Channel Analyser) and a computer was used to record the spectra of different isotopes. The scintillator (or scintillation counter) exploits the atomic excitation produced by a charged particle. Four components make up a scintillator: a light guide, photomultiplier, an electronics circuit to drive the photomultiplier tube (PMT) and the scintillator material (in this case NaI crystal). A γ ray photon incident on scintillator interferes with one of the atoms in the crystal. This interaction causes an electron to be ejected, its energy being for all intents and purposes identical to the incident photon (binding energy of electron is of the order of 10 eV, this can be safely ignored as it is negligible compared to the energy of the inbound γ ray) en-

ergy. This excited electron can ionise other nuclei in the crystal, exciting many more electrons. These secondary excited electrons de-excite, emitting energy in the form of photons (energy losses due to phonon interactions are not considered). These low energy photons (with energies comparable to visible light) are transmitted to the photomultiplier tube via the light guide, where they are converted from optical signals to electrons via the photoelectric effect,which are then amplified. The amplifier consists of a cathode (held at a negative potential by the high voltage power supply) and a positive anode. The electrons that were produced in the PMT via the photoelectric effect are accelerated by this potential towards an anode. During this transition, the electrons collide with dynodes inside the PMT, releasing secondary electrons. The sum of these electrons is interpreted as a voltage pulse, whose energy is proportional to the energy of the incident γ ray.

Recorded data is fed into an MCA, which sorts each voltage pulse according to height, producing a spectrum of energies. Most of the energy is emitted as electrons (inside the PMT), hence the energy of the electrons is equivalent to the energy of the incident γ ray. This results in a photopeak, where the photopeak has the equivalent energy of the γ ray.

Electrons inside the scintillator are produced by three main modes: photoelectric effect, Compton scattering and pair production. The observed spectrum depends greatly on these three processes, as it is the processes that give rise to the peaks, not the gamma rays themselves.

When θ reaches 180 degrees, maximum energy loss occurs, leading to the Compton edge. This Compton edge is easily identified as a sharp drop in counts due to the energy loss in the Compton scattering process. Instead of scattering from an electron the γ ray may scatter from the side of the scintillator first, and only then enter the detector. This results in a backscatter peak, as energy is lost in the scattering between the wall of the scintillator and the γ ray photon.

Gamma ray spectrometers are limited by the resolution of their detectors, which depends on crystal quality inside the scintillator. Resolution(R) can be measured by taking the width at half the maximum of a photopeak (FWHM) and dividing by the energy of the peak, from these measurements the resolution of our scintillator was found to be 11.5%.

$$R = \frac{FWHM}{E} \times 100 \tag{5}$$

To estimate the outcome of our spectra, decay schemes of the isotopes under consideration need to be studied.

Decay processes of ^{137}Cs, ^{22}Na and ^{60}Co

$$^{137}\mathrm{Cs} \rightarrow {}^{137\mathrm{m}}\mathrm{Ba} \rightarrow {}^{137}\mathrm{Ba} + 661.6keV \tag{6}$$

Caesium decays into a metastable state of barium by β^- emission(a neutron decays to a proton, releasing an electron, e^- and an anti-neutrino, $\bar{\nu_e}$). This metastable state has a half life of about two minutes (153 seconds [3]).$^{137\mathrm{m}}$Ba emits a γ ray photon of 661.6 keV to become a stable, ^{137}Ba element.

Compton scattering

An incident γ ray is scattered by an electron through angle θ inside the NaI crystal, losing energy in process. Compton scattering is summarised in the equation below, where $\Delta\gamma$ is the difference between the incident wavelength and the reflected wavelength, m is the mass of the electron.

$$\Delta\gamma = \frac{h}{mc}(1 - \cos\theta) \tag{4}$$

$$^{59}\mathrm{Co} + \mathrm{n} \rightarrow {}^{60}\mathrm{Co} \rightarrow {}^{60}_{28}\mathrm{Ni} + e^- + \bar{v_e} + \gamma_1 + \gamma_2 \tag{7}$$

The metastable ^{60}Co decays via β^- to Nickel, which releases two γ rays of energies 1170keV and 1330keV. These high energy γ rays occur due to a mass difference between ^{60}Co and $^{60}_{28}$Ni of 4.98×10^{-30}kg.

$$^{22}\mathrm{Na} \rightarrow {}^{22}\mathrm{Ne} + \beta^+ + v_e + 1275keV \tag{8}$$

Sodium-22(^{22}Na) decays via β^+ emission ($p \rightarrow n$ emitting an electron neutrino, v_e and a positron, e^+ + energy), emitting a γ ray of 1275keV.

The attenuation coefficient, μ , depends on three processes, each with their own cross section (probability):σ_c(Compton scattering cross section),σ_f(photoelectric cross section) and σ_p (pair production cross section). The total cross section is the attenuation coefficient, μ and is defined by equation 9, [4].

$$\mu = \sigma_c + \sigma_f + \sigma_p \tag{9}$$

For further γ ray absorption information refer to H.Kahn, 'Gamma ray absorption coefficients'. Note that σ_p, the pair production cross section will not be considered here as it only dominates at 5MeV.

$$\sigma_f = \frac{10^{-37} Z^5}{(hv)^{3.5}} \tag{10}$$

At energies comparable to $10 - 1000$ keV, the photoelectric effect is the dominating factor in determining the attenuation coefficient ([4],p 26), the derivation of these formulae can be found in [5].

2 Method

2.1 Gamma ray spectra of ^{60}Co,^{137}Cs and ^{22}Na

In this section γ ray spectra were measured for the radioactive isotopes (^{60}Co,^{137}Cs,^{22}Na) under consideration. The scintillator was calibrated with respect to known γ ray peaks of ^{137}Cs + ^{241}Am The calibration was performed as follows:
^{137}Cs sample was suspended 5cm above scintillator and the spectrum measured over 100 seconds. This was the preliminary measurement. The high voltage was adjusted to give the full spectrum for caesium ($V = 0.84$kV) and the energy calibration was performed via cassylab software, using the photopeak as a reference. Due to the clarity of the caesium photopeak, only this peak was used for the calibration, ^{241}Am was ignored. Once the scintillator was calibrated, radioisotopes were suspended above the scintillator and their spectra measured over 100s. The photopeak was model to a Gaussian fit, to allow the mean value of energy(and therefore the energy of the γ ray) to be calculated. The specific γ ray transitions can be confirmed from [3].

2.2 Measuring the attenuation coefficient of different metals at varying energies

Three metals (aluminium, lead and iron) were investigated at different energies: 661.6keV

At $1000 - 5000$keV Compton scattering is the dominating factor in determining the attenuation coefficient.

$$\sigma_c = Z\sigma_{ce} \tag{11}$$

The Compton cross section (σ_c) is proportional to atomic number for low energies, however it to dominates the photoelectric cross section after 1000keV, at which point an increase in energy decreases the Compton cross section, therefore reducing the attenuation coefficient.

(thin ($0.45 - 1.2$mm) metal samples) and 1253keV(thick($4.8 - 4.88$mm) samples) to confirm the validity of equations 10 and 11. The spectrum was taken first with no absorbers present, gradually adding an absorber every 100 seconds. Gaussian fitting was applied to the photopeak of the metal under consideration, to accurately determine the intensity of the photopeak. The intensity ratio ($\ln I/I_0$) was plotted against thickness to determine the attenuation coefficient for each metal.

Weakly radioactive sources

A weakly radioactive source (KCl salt) was analysed to determine its activity. The sample was encased in a lead cylinder (1.2cm thick) to shield against background radiation. Measurements were taken for 30 minutes and repeated to eliminate anomalous data. The accepted value for the activity of K-40 is taken to be 16000 to 18000 Bq [6], [7]. The activity of a sample is equivalent to the number of disintegrations per unit time,

$$A = \frac{dN}{dt} = \lambda N \tag{12}$$

where N is the number of decays in the sample an λ is the decay constant.

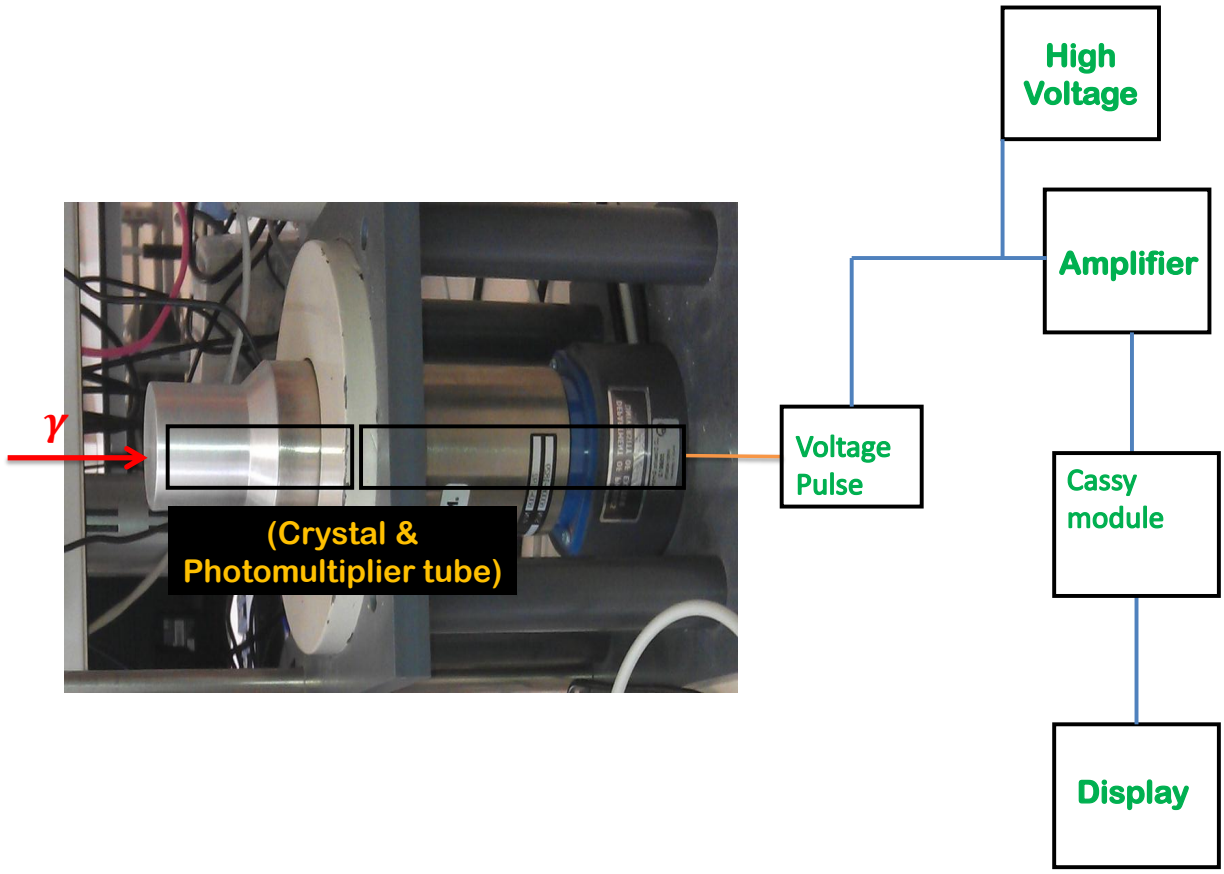

Figure 3: Schematic of experiment. Gamma ray enters the scintillator, where it ejects an electron from the crystal. Since the energy of the γ ray is much greater than the required energy to eject an electron from an atom (typically 10 eV) the electron is detected by the PMT (photomultiplier tube). The ampler amplifies the voltage pulse, which is passed to the MCA (Multi Channel Analyser) present in the cassy module. The corresponding spectrum of counts vs channel number is displayed on the computer screen. This can then be calibrated via software by identifying known peaks.

Radioactivity of different types of coffee

The activity of two brands of coffee were considered. From figure 1, it can be seen that about 12% of the background radiation comes from edible products. The major contribution to this value is the presence of ^{40}K, which is found in bananas, Brazil nuts and other foodstuffs. Compared to bananas or Brazil nuts, there is little scientific data confirming whether coffee is radioactive. According to [8], the typical activity of coffee is approximately 900 Bq. However in [8], samples were left in the marellini beaker for more than a day. Due to time constraints our samples were analysed as a 200 gram source (versus 60 grams in [8]) for 30 minutes. A sodium iodide scintillator was used rather than the (more accurate) germanium crystal scintillator. Activity was measured as an integral at the peak, as this allowed us to measure the radioactivity of the substance due to a particular emission.

3 Results

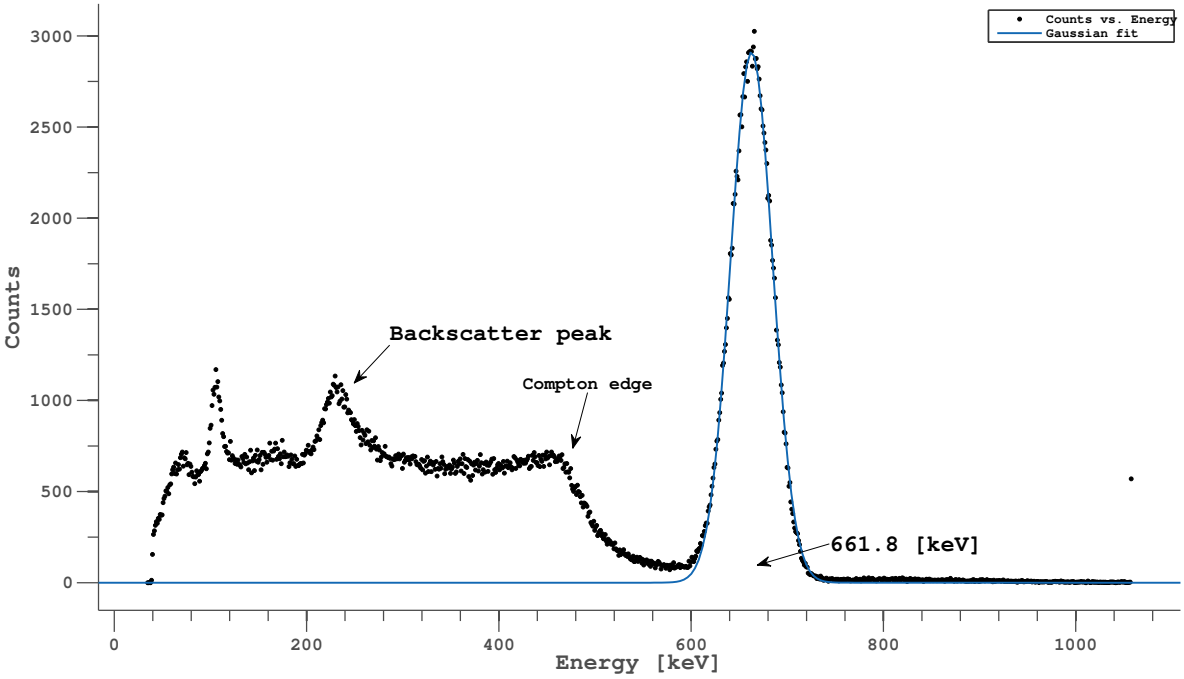

Figure 4: Gamma ray spectrum of ^{137}Cs radioisotope, the peak was observed at 661.8keV, which is which agrees well with theory (accepted value of 662keV).

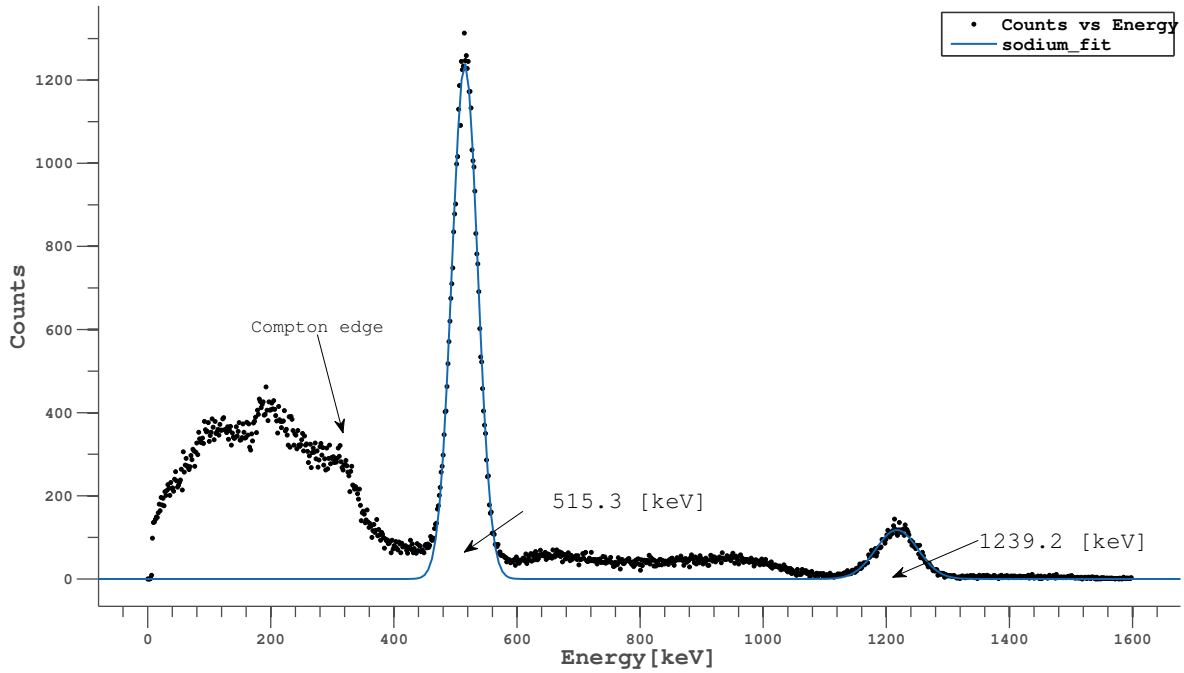

Figure 5: Sodium-22 gamma spectrum, the annihilation peak is clearly identified at 515.3keV (minimum accepted value of 511keV). The peak associated with sodium is found at 1239.2 keV which is within the accepted value (taking resolution errors into account) of 1275 keV

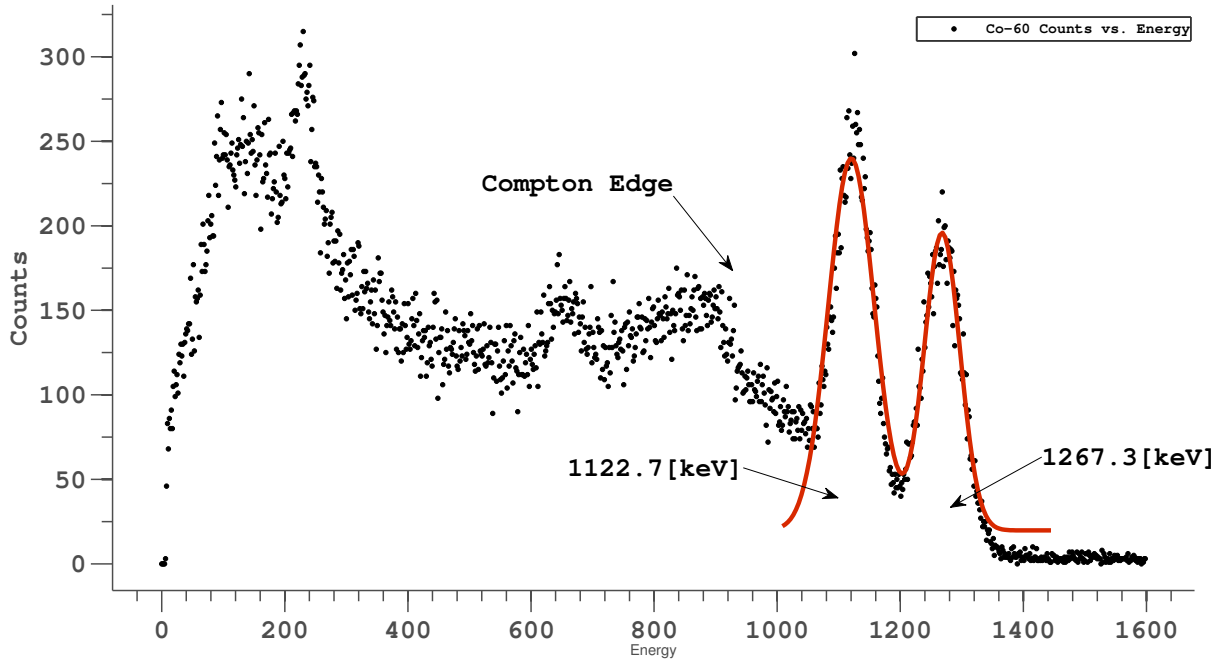

Figure 6: Cobalt spectrum using NaI scintillator. The typical peaks at 1122.7 and 1267.3 are concordant with theory (1170[keV] and 1330 [keV], which is within the resolution error of the scintillator.

Attenuation coefficients of metals at different energies

Attenuation of aluminium was found to be 0.174 ± 0.04[1/cm], which is within the accepted value of 0.16[1/cm]. Similarly the attenuation coefficient for thin lead was found to be 1.03 ± 0.182. The major source of error is due to the non uniformity of thin lead.

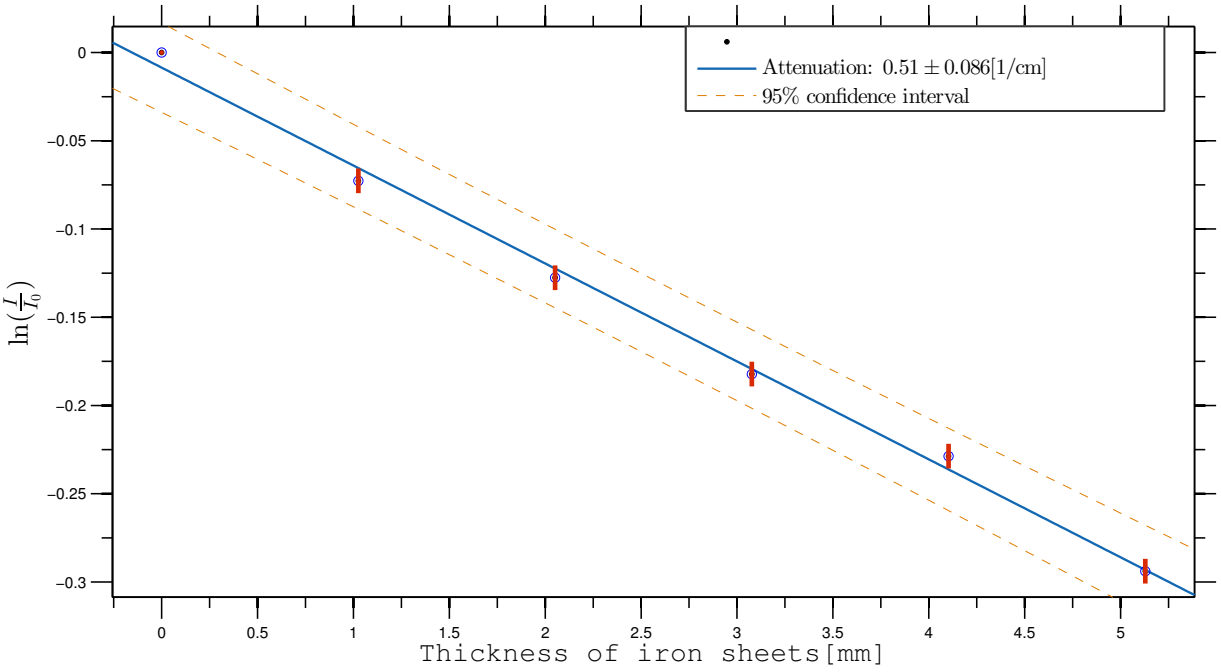

Figure 7: Graph showing the 'Intensity ratio vs thickness plot' for thin iron. The attenuation coefficient was found to be 0.51 ± 0.086[1/cm], which is within the accecpted value of 0.43[1/cm].

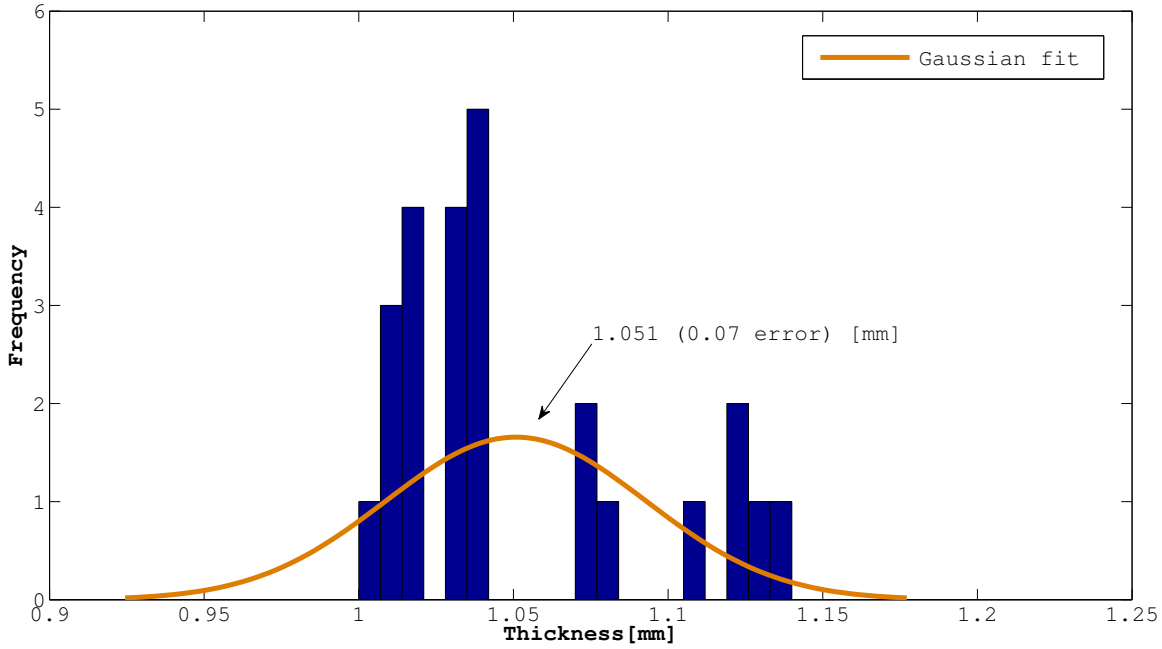

Figure 8: Histogram showing the variation of thickness of thin iron. The mean value was found to be 1.051 ± 0.07 [mm]. Gaussian fitting was applied to evaluate the mean thickness of thin aluminium sheets.

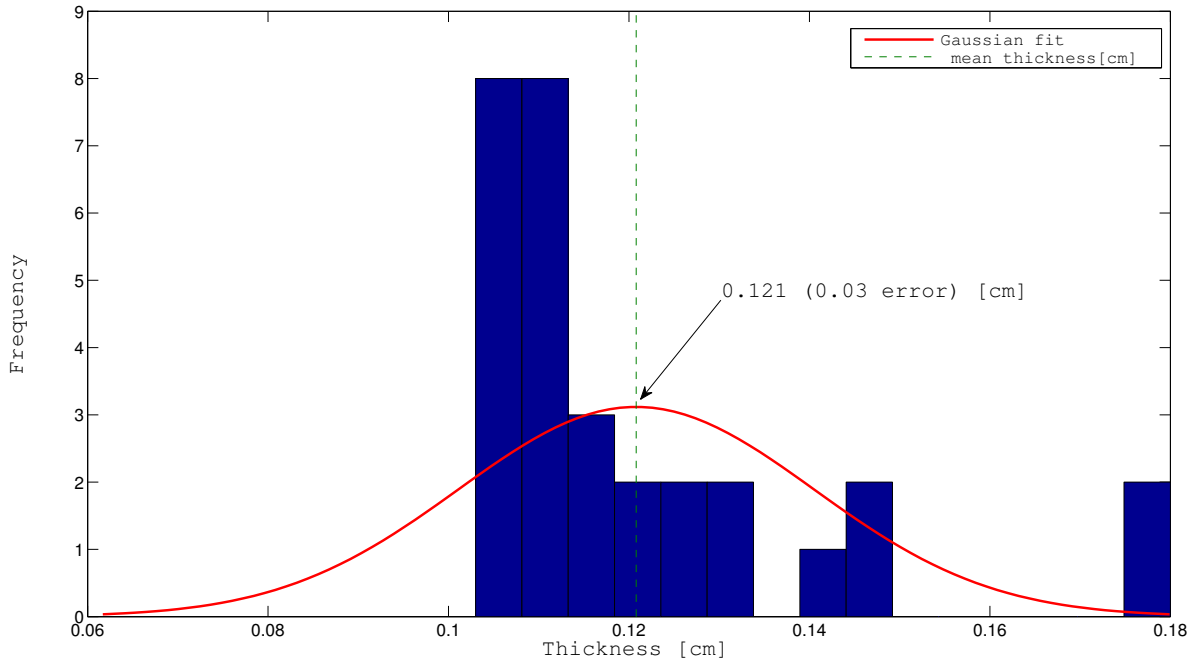

Figure 9: Histogram summarising the thickness measurements for thin lead. The mean value was found to be 0.121 ± 0.03 [cm]. Gaussian fitting was applied to evaluate the mean thickness of the sheets.

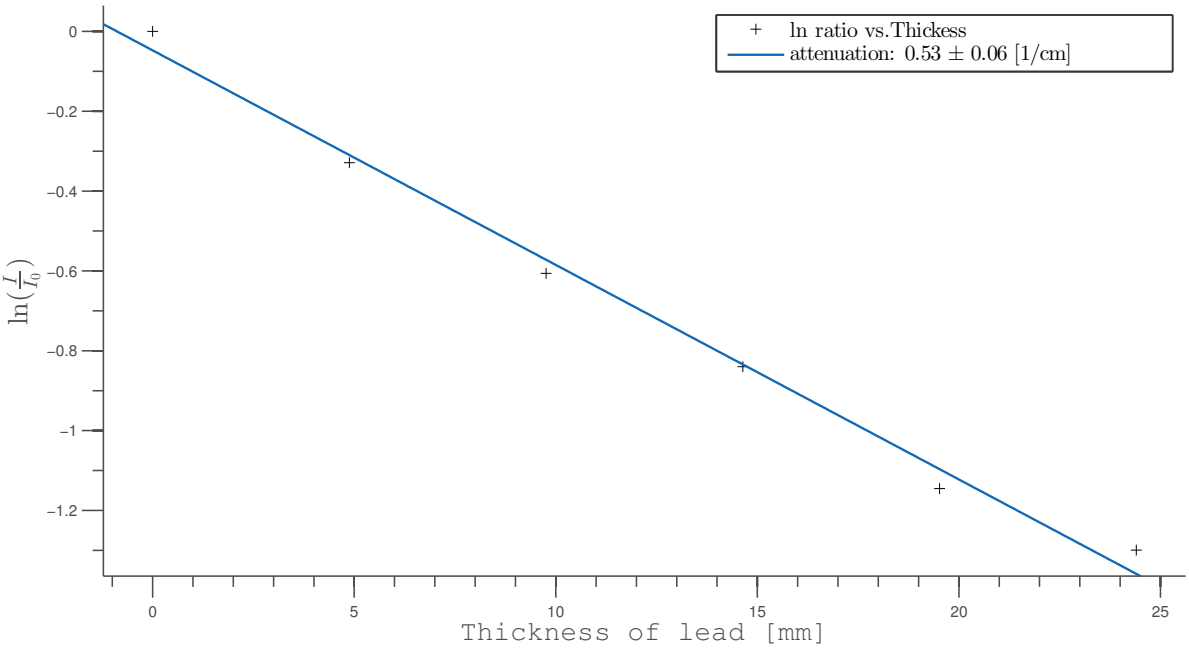

Figure 10: Graph showing the '$\ln(I/I_0)$ vs Thickness' plot for thick lead, using 4.8 mm sheets. The attenuation coefficient was calculated from the gradient, resulting in 0.53 ± 0.06. The error associated with the measurement of the thickness of the sheet is less than 0.01mm, and is therefore ignored as negligible, compared to its thickness.

Similar analysis of aluminium and iron (using 4.8 mm sheets) led to attenuation coefficients of 0.14 ± 0.02 [1/cm] (accepted value of 0.13 cm^{-1} at 1253 KeV) and 0.41 $\pm$ 0.07[cm^{-1}](accepted value of 0.36 [cm^{-1}] at 1253 KeV). Attenuation of thick material was measured using Cobalt-60 as the caesium source is too weak to penetrate more than 1.3cm of lead (the addition of the third block during attenuation measurement). The typical thickness of the metals were found to be 4.8 ± 0.01 [mm], the error associated with the micrometer, and not the variation in thickness of the samples (as was the case with using thin metal sheets).

KCL substance

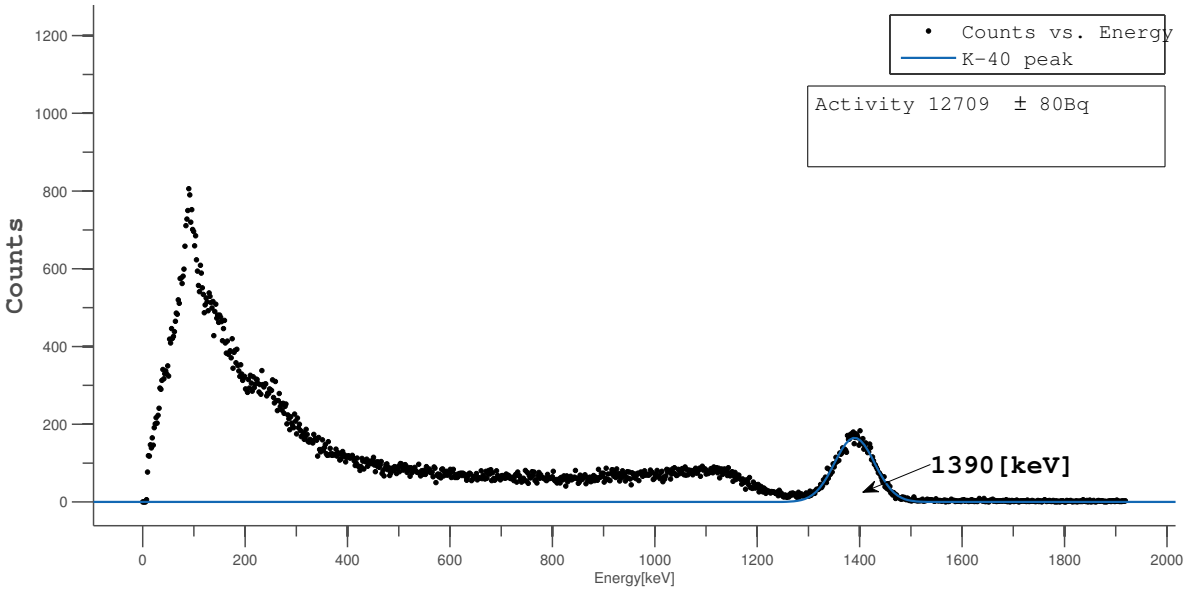

Figure 11: Graph of the gamma spectrum for a potassium chloride salt, the activity of the sample was measured to be 12709 Bq ±80Bq. The activity was measured as the integral of the potassium peak(integral of peak at 1390keV). Bearing in mind that the activity of the sample is reduced from 10 to 40% just by keeping the sample in a plastic container, [9], this value is within the quoted value of 16021 Bq [6] and [7] of 18000±300Bq.

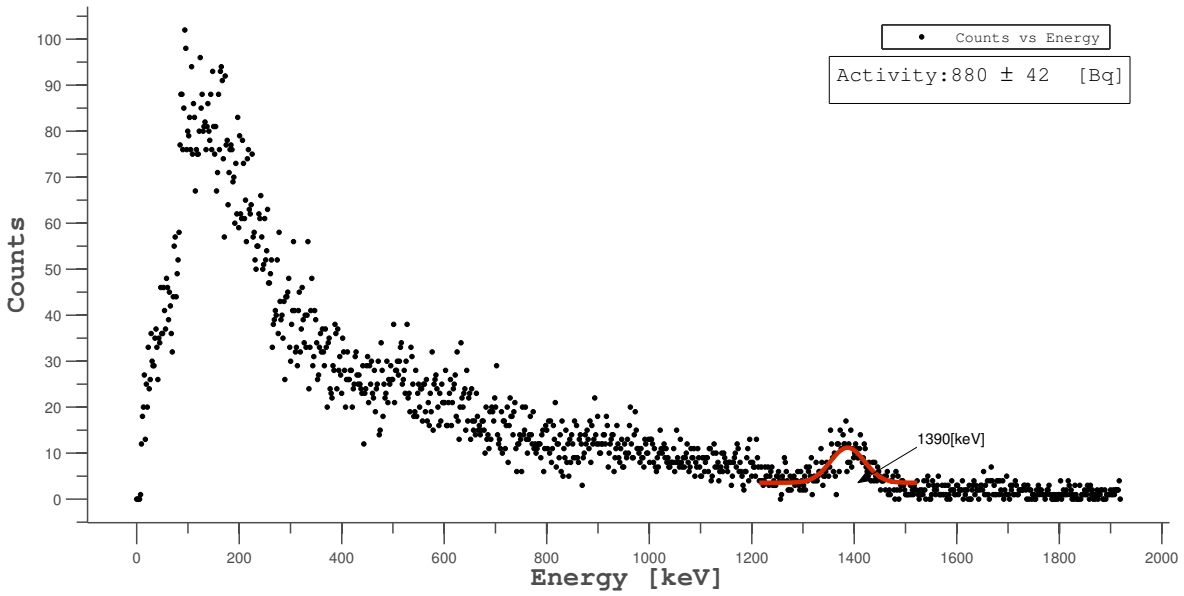

Figure 12: Brazilian coffee radioactivity. A potassium 40 peak can be clearly seen, the activity of the sample is 880 ± 42Bq. This result agrees with previous studies, as the value is within the range specified in [8].

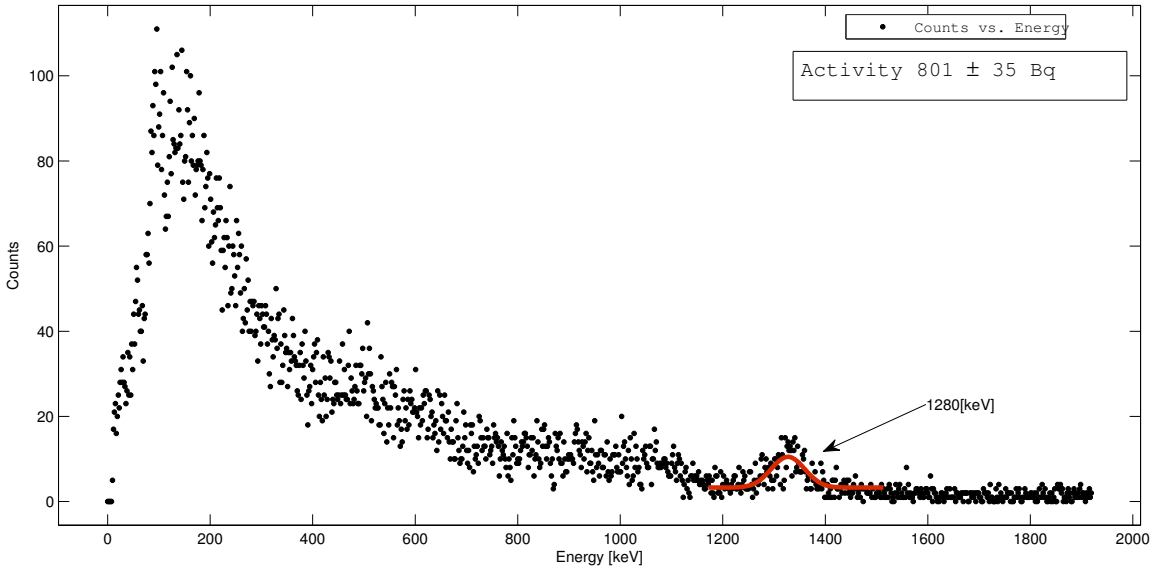

Figure 13: Ethiopian coffee radioactivity. A potassium 40 peak can be clearly seen, the activity of the same is 801 ± 35 Bq.

A visual approach to model thin aluminium sheets

In light of the difficulties of measuring the thickness of thin metal sheets, several readings were taken to form histograms (Figures 8,9) to extract the average thickness of materials. Whilst this did not take a large proportion of our time, it gave us an idea whether this monotonous task can be done more effectively if automated. The reason for having a more visual model was to confirm whether this method could be used if the sample is too cumbersome to analyse manually (for example if it requires many hundreds of readings) or when it is otherwise preferential to give an image-like output of the measurements.

The procedure to create the thickness plot (page 12) required 2 high resolution images (of all aluminium sheets arranged in a square), taken at different angles. This allows the program to recreate a three dimensional model of the sample. These

images were then imported into Blender [10] with which a 3D model was generated. This reduced the time taken for the model to be generated, as only one 3D surface can be considered. This data was then imported into MATLAB and plotted. This method can potentially simplify data acquisition when a large number of readings need to be performed, however this procedure took almost 9 hours to finish (due to limitations in computational power available), a result which would improve dramatically on a more capable system. The outcome is a surprisingly accurate representation of the thicknesses (**not** the visual appearance) of aluminium sheets, which can be seen on page 12, Figure 14.

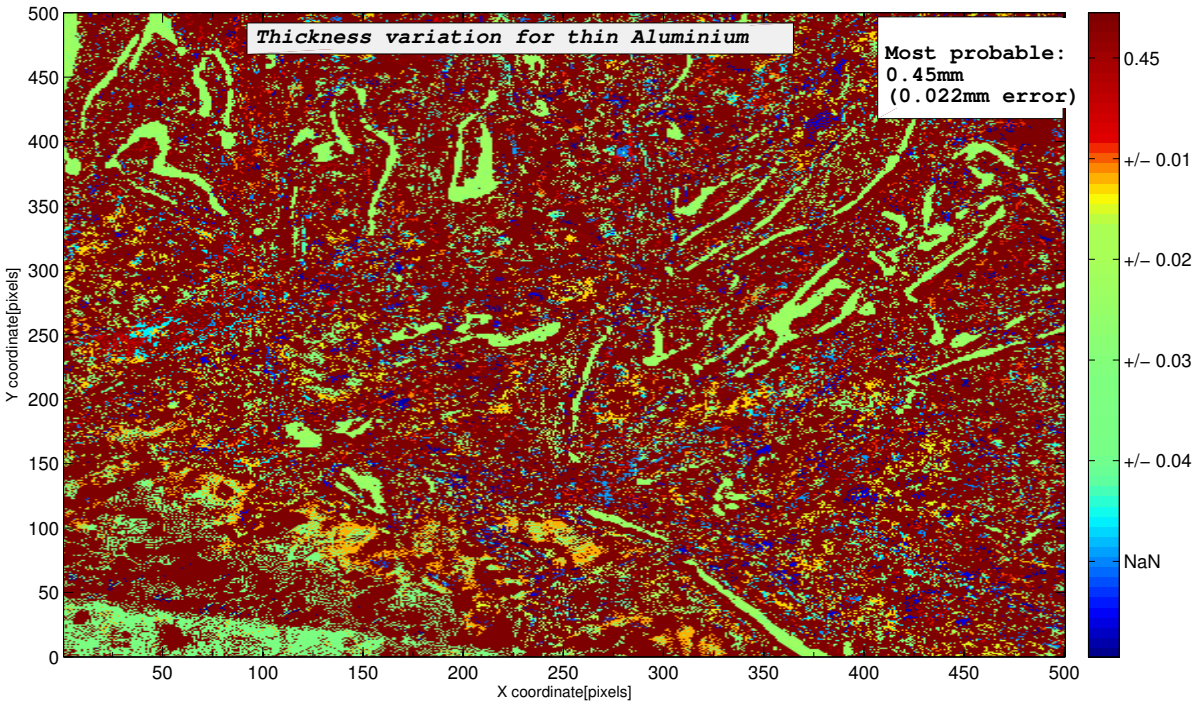

Figure 14: MATLAB generated image of the thickness of the aluminium sheets. This model was confirmed by measuring the thicknesses of the aluminium sheets at random positions several times and averaging the result (via a Gaussian fit). The blue regions are indicative of the limitation of the model to deal with external interference (in our case camera flash) and were ignored in the average thickness measurement. The average thickness of the aluminium sheet was found to be 0.45 ± 0.22 mm. This model was confirmed by manually measuring the thicknesses of the aluminium sheets. This gave a result of 0.44 ± 0.24 mm

4 Analysis

The largest error associated with the γ ray spectra is the comparatively low resolution of the detector(11.5%). Another contribution to the error was the fluctuation of the high voltage supply (noted to be $\pm 50 - 80$ V), causing the peak to broaden at its maximum (as the energy calibration changes with changing high voltage).
The activity of the two types of coffee can be interpreted as high (especially if one considers that the background count is only 80 Bq), however when the spectrum was analysed, it was found that coffee contains Potassium-40, a common radioisotope found in soil. This particular isotope has a very long half-life (10^9 years), but is quickly removed from the human body (typically $8 - 10$ hours), hence poses little risk as far as radiation doses are concerned. The attenuation coefficients for thin aluminium, lead and iron are concordant with theory. It is clear that coffee is radioactive, however the radioisotope present in the two brands of coffee studied is harmless and is present in many other foods (bananas, brazil nuts etc). Measurements for Brazilian and Ethiopian coffee was performed without its original aluminium foil packaging, producing results only with minor deviation($10 - 30$ counts). To evaluate this problem further a more accurate germanium detector can be used with conjunction of extra shielding (for example using concentrated bromide solution). The activity of the KCL sample was measured to be 12709 Bq which is comparable to independent data, when absorption due to plastic shielding is taken into account.

A discrepancy was noted between KCL salt spectra and coffee spectra (Figures,11,12, 13 pages 10 through 11). A peak at 178 keV was noted in all three measurements. Originally it was considered that this was a ^{14}C peak, with an activity of 2209 ± 49 Bq in the coffee samples. The presence of C-14 is justified in coffee as it is the basic building block of every landborne organism. The ratio of Carbon-14 (concentration of C-14 with respect to carbon 12) in coffee was calculated to be approximately 1.3×10^{-10}, almost equivalent to the accepted value of 1.0×10^{-10}, [11]. However, this was not concordant with measurements for a KCl salt, since there is no reason for a ^{14}C peak to be present in the sample.

According to [12], ^{40}K decays primarily by β^- emission(90%), from 560.2keV to 1311keV, and rarely (10%) emitting a γ ray of 1460.8 keV. All three graphs confirm the γ emission peak.

Upon closer examination it was concluded that from 200 to 900 keV the curve fitted the Fermi theory of β decay [13]. The shape of the peak is an interesting consideration for physicists, as it allows us to obtain angular momentum information. β emission is a wide spectrum emission, as each positron or electron can have a range of kinetic energies. The conservation of linear momentum and energy leads to the conclusion that in β decay a third particle (electron neutrino) must be produced. According to [14], the peak present in figures 11 to 13 is indeed a positron emission peak.

5 Conclusions

It was found that a calibrated NaI scintillator outputs results withing 11.5% of the accepted values. The photopeaks for ^{60}Co,^{137}Cs,^{22}Na were found at 1122.7 and 1267.3,(^{60}Co) keV, 661.8keV , (^{137}Cs, accepted value 661.8 keV) keV, and 515.3 and 1239,(^{22}Na) keV. The values for the energies of the photopeaks were within the accepted range of values, taking into account error due to the low resolution of the NaI scintillator($\pm$11.5%). The attenuation coefficients for thin and thick materials are summarised in the table below.

Material	Thickness	Energy[keV]	μ[1/cm]$\pm$ error	μ theory[1/cm]
aluminium	thin	662	0.174 ± 0.04	0.16
aluminium	thick	1253	0.14 ± 0.02	0.13
iron	thin	662	0.51 ± 0.086	0.43
iron	thick	1253	0.41 ± 0.07	0.36
lead	thin	662	1.03 ± 0.182	0.86
lead	thick	1253	0.53 ± 0.06	0.55

The radioactivity of Brazilian and Ethiopian coffee was calculated to be 880 and 801 Bq respectively, which is within the values quoted in [8]. A model was suggested to measure the thicknesses of materials, which gave surprising accurate results. This model could be further used in mapping thicknesses of different materials in future studies.

References

[1] The Mars Odyssey Gamma-Ray Spectrometer Instrument Suite W.V. Boynton, W.C. Feldman, et al

[2] http://2012books.lardbucket.org/books/general-chemistry-principles-patterns-be680db1e491jpg

[3] http://nucleardata.nuclear.lu.se/toi/

[4] Siegbahn, β and γ ray spectroscopy, pp26-80

[5] W. Heitler, Quantum theory of radiation (pp 82-84).

[6] Activity of potassium, p271 Cassy documentation,

[7] Decay of K40,Engelkemeir, D. W.

[8] Radioactivity in coffee C. Roselli, D. Desideri et al, Budapest July 2012

[9] Beta radiation shielding with lead and plastic, Van Pelt WR, Drzyzga M.2007

[10] http://www.blender.org/

[11] http://www.c14dating.com/int.html

[12] http://www.nndc.bnl.gov/nudat2/decaysearchdirect.jsp?nuc=40K&unc=nds

[13] Siegbahn, γ ray spectroscopy, chapter 9 (by M.E.Rose)

[14] Background model for a NaI (Tl) detector devoted to dark matter searches S. Cebrina, b, C. Cuestaa, b, et al

[15] Halliday, Introductory Nuclear Physics (Chapters 4-8)

[16] Supian Bin Samat et al , Activity of one gram of potassium

[17] http://www.ehs.msu.edu/ , carbon-14 data